

About laser heat absorbing impurities in the transparency matrix of pentaerythritol tetranitrate

G Murastov, V Tshipilev, V Ovchinnikov and A Yakovlev

National Research Tomsk Polytechnic University, 30 Lenin Ave., 634050, Tomsk, Russia

E-mail: murastov.gennadiy@gmail.com

Abstract. Simulation of laser heat absorbing inclusions in a transparent matrix of explosive material is carried out. The inclusions are spherical particles with R_0 radius ranging from 10^{-5} to 10^{-2} cm. The duration of the laser pulse varies from 10^{-9} to 10^{-3} s and allows investigating process in both adiabatic and quasi-stationary heating modes. It has been found that the duration of laser pulse affects the maximum heating temperature for particles with a specific radius. A remarkable thing is that the temperature drastically decreases if the absorption cross section and small size of inclusions are taken into account. It leads to heat reduction in a thermal center, which is formed nearby a small-sized inclusion, and shows strongly decreased reactive capacity of explosive decomposition.

1. Introduction

Heat absorbing irregularities in a transparent matrix of explosive material (EM) have been studied previously to solve the problem of ignition of lead azide with different laser pulse duration [1,2]. It was assumed that lead particles are present in the matrix of explosives and laser pulse energy is stored in the particle volume. The critical heat storage in the center and temperature in its vicinity were calculated numerically in a wide range of laser pulse duration in terms of the thermal microcenter model of initiation from the adiabatic mode to the quasi-stationary mode.

The process of heating lead azide particles in the matrix was analyzed. Formation of heat centers ("hot spots") in unreactive medium was addressed in [3]. The features of heating inclusions with different size were shown. The maximum achievable values for surface temperatures of inclusions of different size were calculated numerically and analytically. The temperature profiles of heating in the vicinity of the particles were evaluated for a range of "short" and "long" laser pulses. And these features must be considered in both simulation of laser initiation and interpretation of the numerical calculation results.

Experimental works on laser initiation of PETN are considered to be of great interest nowadays [4–10]. A number of works report on PETN containing no inclusions [4–7] and provide experimental results for PETN containing inclusions of nano-sized carbon particles [9,11] or different metal particles [8,10]. It has been shown that nano-sized carbon additives and aluminum particles lead to 5–6 fold decrease in the initiation threshold. It seems to be interesting that the decrease for carbon impurities and aluminum impurities is similar despite strong differences in their optical performance and thermal performance, as well in chemical activity.



In-depth insight in the nature of laser initiation of composites based on PETN requires the study of the heating process of impurities of different nature exposed to laser beam. It is assumed that the matter is an unreactive medium. This question is the subject of this report.

2. Numerical simulation

Numerical simulation of laser heating of absorbing particle is conducted by the method described in [1,2], and it is assumed that the absorption cross section of the particles in the matrix of explosives does not correspond to geometric one. Illumination on the surface in numerical simulation is different from that produced on the sample surface by laser beam. Following [2], the temperature ΔT :

$$\Delta T \sim k \cdot F \cdot H_{\Pi}, \quad (1)$$

where $k = \frac{\sigma}{\pi \cdot R_0^2}$; $\sigma(R_0, \lambda_0, n_0, n_k)$ is absorption cross section [12] of the particle depending on

radius R_0 , laser wavelength λ_0 , n_0 is refractive index of the medium and n_k is complex refractive index of the absorbing particles; $F = \frac{H_0}{H_{\Pi}}$; H_{Π} is the energy density on the EM surface; $H_0(d_{\Pi}, \mu, \beta, \chi)$

is the energy density in the vicinity of the particles; for the general case, it depends on the size d_p of the laser beam on the sample surface, μ is absorption parameter and β scattering parameter, χ is scattering indicatrix of elementary volume.

Thus, k is the effective absorption coefficient of the particles. The relation between the spatial illuminance within the medium volume and the illuminance of the incident laser flux on the surface are expressed by F . Having normalized (1) to $k \cdot F$ and $H_{\Pi} = q_{\Pi} \cdot \tau$, we obtain:

$$\frac{\Delta T}{k \cdot F} \sim H_{\Pi} = \sigma \cdot \tau, \quad (2)$$

where q_{Π} is laser flux density (W/cm^2).

The heating model takes the form from [2] in case of $\alpha_1 \gg \alpha_2$

$$\begin{cases} \frac{\partial T_1}{\partial t} = \frac{3 \cdot \alpha_2 \cdot c_2 \rho_2}{R_0 \cdot c_1 \cdot \rho_1} \cdot \frac{\partial T_2}{\partial r} + \frac{3 \cdot q_{\Pi}}{4 \cdot R_0 \cdot c_1 \cdot \rho_1} \\ \frac{\partial T_2}{\partial t} = \alpha_2 \cdot \frac{1}{r^2} \frac{\partial}{\partial r} \left(r^2 \frac{\partial T_2}{\partial r} \right) \end{cases} \quad (3)$$

where T_1 is the temperature of the particle; T_2 is the EM temperature; c_1 is the specific heat capacity of the particle; ρ_1 is the density of one particle; c_2 is the specific heat capacity of explosive; ρ_2 is the density of explosive; r is the coordinate of the heating point in a spherical coordinate system; R_0 is the radius of the particle; α_1 , α_2 are thermal conductivity of particles and explosive material, respectively; q_{Π} is the laser flux density.

The solution of (3) was performed for different duration of the heating pulse and constant H_{Π} value equal to $100 \text{ mJ}/\text{cm}^2$, which is close to the experimental value obtained in [2]. The threshold power density was measured for a pure PETN sample (no impurities) with laser pulse duration of 10 ns. The pulse was Π -shaped in all the studied range of pulse widths. It is the best to suit the structure of long laser pulses in the region where the pulse waveform affects the result of heating [1,2]. The particle taken was spherical.

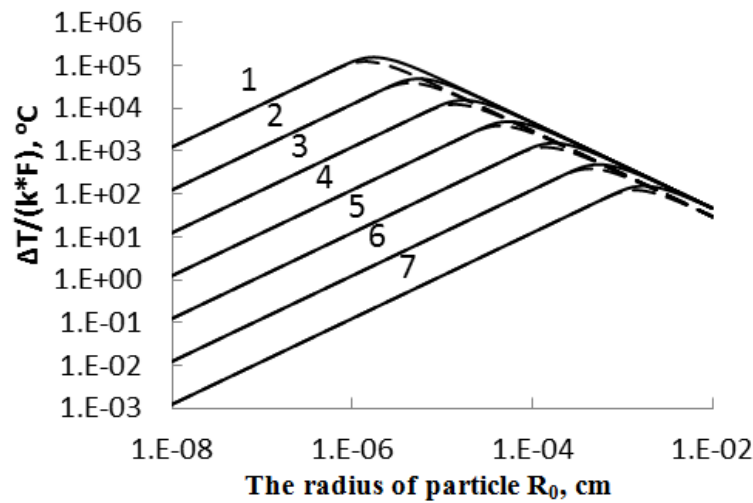


Figure 1. Dependence of the specified heating temperature of spherical carbon particle (solid curves) and aluminum particle (dotted line) on radius R_0 . The energy density on the surface of the compacted PETN powder $H_{\Pi}=100\text{mJ}/\text{cm}^2$. The duration of the laser pulse $\tau=10^{-9}\text{s}$ (1); 10^{-8}s (2); 10^{-7}s (3); 10^{-6}s (4); 10^{-5}s (5); 10^{-4}s (6); 10^{-3}s (7).

The following constants were used for calculation $c_1=760\text{ J/kg}\cdot\text{K}$; $\rho_1=2250\text{ kg/m}^3$; $\alpha_1=9.6\cdot 10^{-7}\text{ m}^2/\text{s}$; $c_2=1672\text{ J/kg}\cdot\text{K}$; $\rho_2=1700\text{ kg/m}^3$; $\alpha_2=6.67\cdot 10^{-8}\text{ m}^2/\text{s}$.

The results of numerical calculations of ΔT particle heating for a wide range of laser pulses duration and sizes of carbon particles and aluminum particles are shown in figure 1. The set of curves on the scale $\frac{\Delta T}{k \cdot F}$ is of equal shape for carbon particles (solid curves) and for aluminum particles (dashed lines). The general patterns for particle heating are observed to be independent of the material used. First of all, each of the pulse durations corresponds to the particle size which exhibits best heating. Thus, the maximum heating point for carbon particles with $R_0 \sim 100\text{ nm}$, $\tau=1\text{ }\mu\text{s}$ – $R_0 \sim 500\text{ nm}$ and $\tau=1\text{ ms}$ – $R_0 \sim 20\text{ }\mu\text{m}$ in case of laser pulse $\tau=1\text{ ns}$. For aluminum particles, the pattern is similar, but the radius of the particles, wherein the maximum heating is realized, is somewhat less than that of carbon particles.

In the range of small particle size, the temperature of impurity increases linearly with increasing size R_0 . This behavior corresponds to quasi-stationary heating ($\frac{\Delta T}{k \cdot F} \sim R_0$). The region becomes wider with increasing τ (figure 1, the left branch of the curves). At high values ($R_0 > 10^{-5}\text{ cm}$), adiabatic mode is realized: $\frac{\Delta T}{k \cdot F} \sim \frac{1}{R_0}$, ΔT decreases with increasing R_0 (figure 1, the right branch of the curves).

The exact expressions for the heating temperature in asymptotics of these modes are shown in [3]. The formula for adiabatic heating mode is:

$$\frac{\Delta T}{k \cdot F} = \frac{3 \cdot q_{\Pi} \cdot \tau}{4 \cdot R_0 \cdot c_1 \cdot \rho_1} = \frac{3 \cdot H_{\Pi}}{4 \cdot c_1 \rho_1 \cdot R_0}, \quad (4)$$

for stationary heating mode, it is:

$$\frac{\Delta T}{k \cdot F} = \frac{q_{\Pi} \cdot R_0}{4 \cdot \lambda_T}, \quad (5)$$

where λ_T is the thermal conductivity of the matrix.

It should be noted that expressions (4) and (5) can be used to check the accuracy of numerical calculations.

Thus, ΔT peak position for specific pulse duration τ conditionally divides the fields of stationary and adiabatic heating modes.

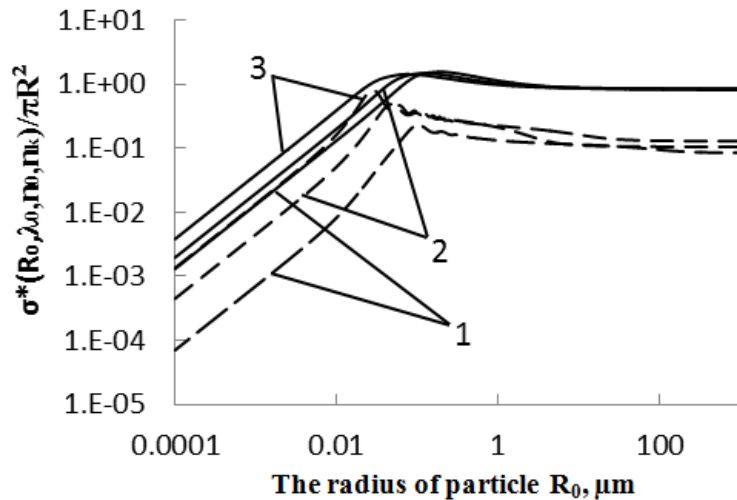


Figure 2. Dependence of the relative absorption cross section of carbon particles (solid curves) and aluminum particles (dashed lines) in the PETN matrix on radius R_0 . The wavelength of laser is 1064 nm (1); 532 nm (2); 354.7 nm (3).

The issue of theoretical and practical interest is the heating curve taking into account the coefficients k and F . To determine the impact of the coefficient k , we calculated values using the expressions from Mie theory for aluminum and carbon particles in the range of R_0 sizes (wavelengths of laser radiation are 1064 nm, 532 nm and 354.7 nm that correspond to 1st, 2nd and 3rd harmonics of neodymium laser radiation and correspond to the PETN matrix transparency region[13]). The values of the complex refractive indices of carbon and aluminum particles were taken from [14,15] and accounted for the first harmonic $2.49-0.015i/1.028-9.25i$; for the second harmonic $2.558-0.025i/0.727-5.663i$ and for the third harmonic $2.684-0.091i/0.291-3.717i$, respectively. The calculation results are shown in figure 2. It can be seen that for both types of inclusions the relative absorption cross section decreases sharply with decreasing R_0 , since $R_0 \sim 10^{-5}$ cm. For $R_0 > 10^{-5}$ cm (100 nm), the absorption cross section weakly depends on R_0 , and for specified R_0 , the k value may be greater than one. For each of the wavelengths, the maximum value k is generated (the first Mi extremum), and its position is shifted towards its reduction. For carbon particles, the maximum k attains the values $R_0=200$ nm, $R_0=160$ nm, $R_0=70$ nm for the 1st, 2nd and 3rd harmonics, respectively; for aluminum particles, the position of the maximum corresponds to the values $R_0=100$ nm, $R_0=60$ nm and $R_0=40$ nm. It can be assumed that the absorption cross section of the particles can have a significant influence on heating especially that of small-sized particles.

Figure 3 shows the results of calculations for the temperature of heating the particle surface with the values $k(R_0, \lambda_0, n_0, n_k)$ and $F(d_{II}, \lambda_0, n_0, P_{np}, \chi, \mu, \beta)$. The value of $F \approx 10$ was calculated for the case of wide laser beam using methods provided in [8]. It weakly depends on the considered wavelengths. The analysis of figure 3 shows that the basic patterns associated with maximum heating of a specified particle size for a given pulse duration remain unchanged. For carbon particles for $\tau=10$ ns, the maximum temperature is observed in particles with $R_0=100$ nm, $R_0=80$ nm and $R_0=50$ nm upon irradiation with 1st, 2nd and 3rd harmonics, respectively. For the maximum heating point of aluminum particles, the size is $R_0=80$ nm, $R_0=50$ nm and $R_0=65$ nm, respectively. In the region of large values of

R_0 , an adiabatic heating mode ($\Delta T \sim 1/R_0$) prevails; however at low values of R_0 ($R_0 < 100$ nm) accounting the absorption cross section the curve shape sharply changes so that in this region $\Delta T \sim R_0^2$. Thus, at constant energy of the laser pulse of different duration, we observe complex dependence of the heating temperature for absorption centers of different nature and, hence, the heat stored in the hot spot, on the size of these centers.

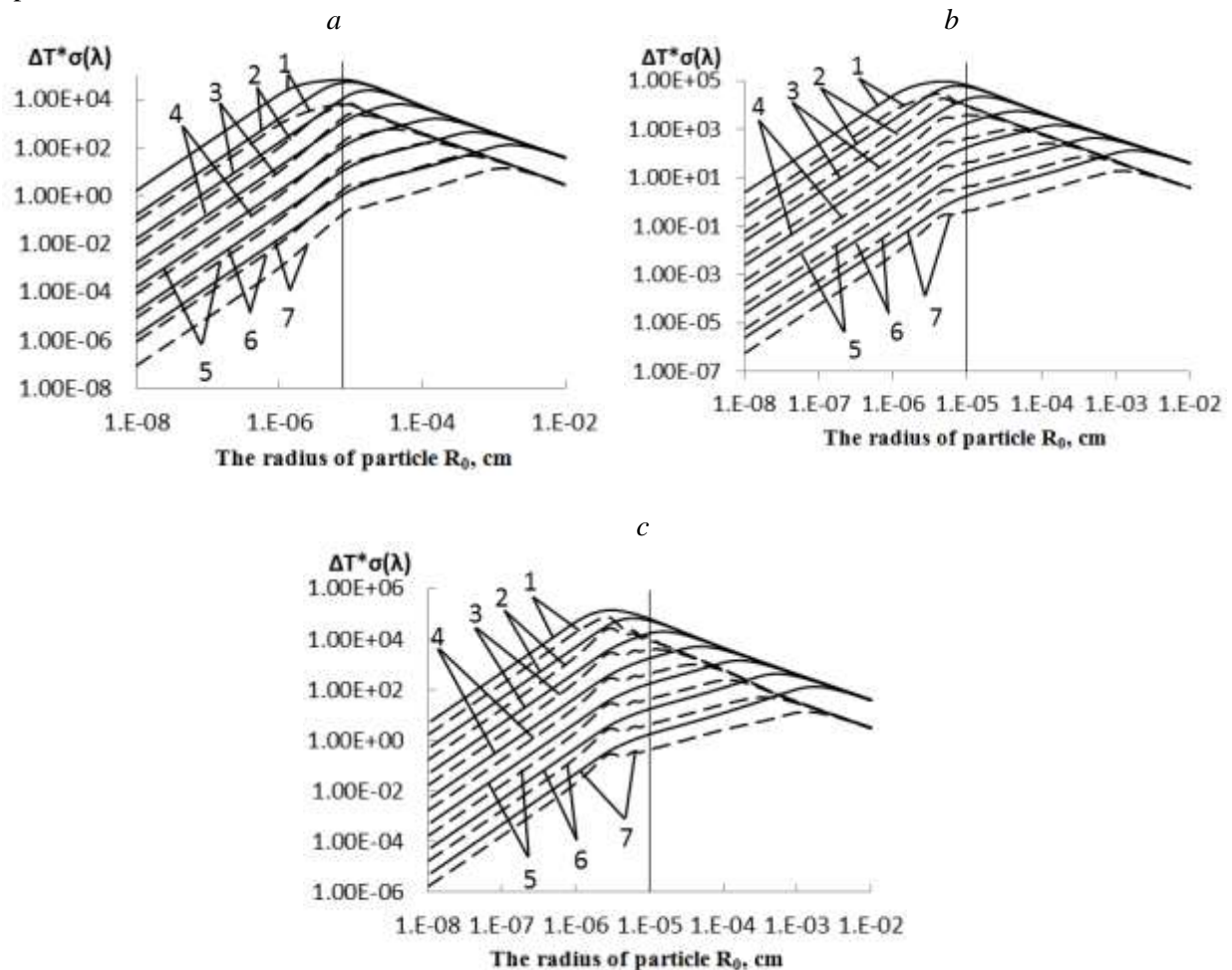


Figure 3. The dependence of the heating temperature on R_0 taking into account $k(R_0)$ at $\lambda_0=1064$ nm for carbon particles (solid curves) and aluminum particles (dotted line) in the PETN matrix. *b* is the dependence for $\lambda_0=532$ nm; *c* the dependence $\lambda_0=354.7$ nm. The laser pulse duration τ : 10^{-9} s (1); 10^{-8} s (2); 10^{-7} s (3); 10^{-6} s (4); 10^{-5} s (5); 10^{-4} s (6); 10^{-3} s (7)

The heat storage Q in carbon particles and aluminum particles in the centers and in their neighborhood ($Q = k \cdot F \cdot H \cdot \pi \cdot R_0^2$) is shown in figure 4 for a wavelength of 1064 nm. Heat storage in the center does not depend on the heating mode, and is proportional to R_0^2 ; however for small R_0 ($R_0 < 10^{-5}$ cm), relative absorption cross section $k(R_0) \sim R_0$, which changes the dependence $Q(R_0)$, i.e. $Q(R_0) \sim R_0^3$, and it sharply decreases with R_0 reduced. This poses an ambiguous question about the reactivity of the centers. According to the adiabatic heating mode, as R_0 decreases, reactivity increases and then decreases sharply when $R_0 < 10^{-5}$ cm. In this mode, the criterion for initiation from data in [2] is to achieve a certain critical value of heat storage in the center. This value decreases monotonously with R_0 reducing. However, at first with reducing R_0 , the reactivity increases but then at $R_0 < 10^{-5}$ cm, it sharply decreases [1].

In terms of the quasi-stationary mode, the heating initiation criterion is a specified critical temperature achieved in the center [2]. At the same time, the temperature of the center increases with R_0 growing (figure 1), the heating zone h ($h \approx R_0$) grows, and accordingly, their reactivity increases, which is confirmed by numerical calculation data [3] on ignition of lead azide. Note that in this mode, the heat storage in the absorbing particle is different and proportional to $k \cdot F \cdot H \cdot R_0^4$

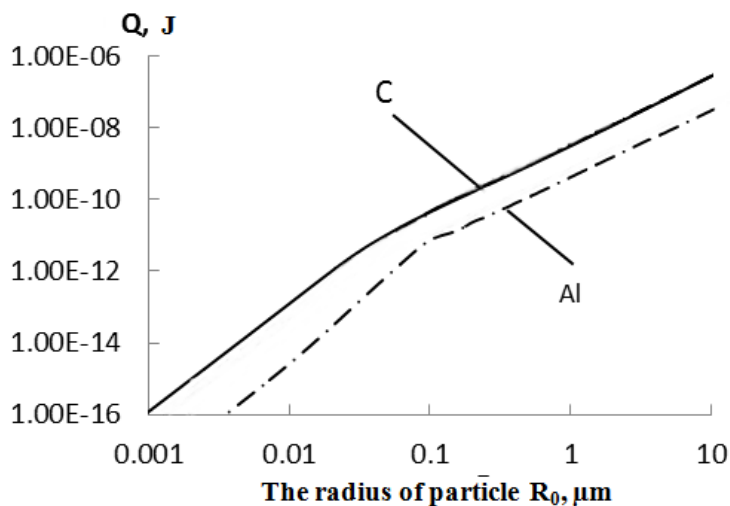


Figure 4. The heat storage near the aluminum particle (dotted line) and carbon particle (solid curve) depending on radius R_0 at energy density of the laser pulse up to 100 mJ/cm^2 for the wavelength $\lambda_0=1064 \text{ nm}$.

3. Conclusion

The analysis of the results revealed a number of patterns of laser heating:

1. Micro- and nanoparticles of the carbon and aluminum impurity can be heated up to the values of tens of thousands degrees under laser pulse irradiation of mixed compositions based on PETN powders at near threshold levels of exposure ($\sim 100 \text{ mJ/cm}^2$). At the same time, the values of carbon particle heating can exceed those of aluminum heating by one order of magnitude.

2. For the impurity particles of different nature (carbon, aluminum) and for specified pulse duration, there is a certain size at which these are heated most. For experiments with laser pulse duration of about 10 ns, the maximum temperature for carbon particles is achieved for particles with size $R_0=100$, $R_0=80$ and $R_0=50 \text{ nm}$ at an irradiation wavelength of 1064, 532 and 354.7 nm, respectively. For aluminum particles, the maximum heating point is observed for $R_0=80$, $R_0=50$ and $R_0=25 \text{ nm}$, respectively.

3. In case of $R_0 < 100 \text{ nm}$, a quasi-stationary particle heating mode at $\Delta T \sim R_0$ can be observed in the entire investigated range of laser pulse durations. In case of $R_0 > 1 \mu\text{m}$, an adiabatic heating mode is generally observed, where $\Delta T \sim 1/R_0$. These characteristics determine the amount of heat in the microcenter formed in the vicinity of inclusions of different radius R_0 , and their further development in the centers of explosive decomposition.

These patterns and features must be considered in theoretical and experimental studies of the sensitivity of mixed composition, as well as explosives containing intrinsic optical inhomogeneities, to the pulsed laser radiation.

It should be noted that the calculations were carried out through solid-phase approach without taking into account melting and evaporation of explosive matrix and impurity particles, which simplifies the calculation and analysis of the results but leads to overestimated values of the heating temperature. Furthermore, for the smallest values $R_0 < 10^{-7}$, the description of absorption and scattering

processes may differ from that made under the Mie theory. However, not quantitative but qualitative patterns of the heating process are the issues of most interest in this paper.

Note that taking into account the chemical reaction in the vicinity of inclusions can provide a more accurate pattern of center heating and, in particular, specify the data on heat store in the centers and their reactivity. Further studies of the issue will be performed.

Acknowledgments

This work was financially supported by the Russian Foundation for Basic Research Grant 15-03-05385.

References

- [1] Aleksandrov E, Sidonskii O and Tsipilev V 1991 Influence of combustion in the vicinity of absorbing inclusions on the laser ignition of a condensed medium *Combustion, Explosion, and Shock Waves* **27** pp 267–272
- [2] Aleksandrov E and Tsipilev V 1984 Effect of the pulse length on the sensitivity of lead azide to laser radiation *Combustion, Explosion, and Shock Waves* **20** pp 690–694
- [3] Morozova E, Tsipilev V and Burkina R 2011 Initiation of reactive substances radiation flux at its absorption optical inhomogeneities of matter *Combustion, Explosion, and Shock Waves* **47** pp 95–105
- [4] Tsipilev V 2001 Laser initiation of PETN *Physico-chemical processes in inorganic materials* (Kemerovo) pp 113–114
- [5] Zinchenko A and Tarzhanov V 1996 Laser initiation of PETN *Combustion, Explosion, and Shock Waves* **32** pp 113–119
- [6] Karabanov Y and Bobolev V Burning of solid secondary explosives short pulse lasers *Combustion of Condensed Matter* (Chernogolovka) pp 5–8
- [7] Skripin A, Morozova E and Tsipilev V 2010 Laser initiation of PETN powder in a volume compression *Bulletin of the Tomsk Polytechnic University. Energetic* (TPU, Tomsk) **317** pp 149–155
- [8] Aleksandrov E, Voznyuk A and Tsipilev V 1989 Effect of absorbing impurities on explosive initiation by laser light *Combustion, Explosion, and Shock Waves* **25** pp 1–7
- [9] Aduiev B, Nurmukhametov D, Furega R, Zvekov A and Kalensky A 2013 The explosive expansion of PETN with nanoadditives aluminum when exposed to pulsed laser radiation of different wavelengths *Chemical Physics* **32** pp 39–44
- [10] Aduiev B, Nurmukhametov D, Furega R and Zvekov A 2014 Regulation of PETN sensitivity to laser exposure via nanoparticle additives metals nickel and aluminum *Chemical Physics* **33** pp 37–41
- [11] Ovchinnikov V, Skripin A, Tsipilev V and Yakovlev A 2012 Dependence of explosion initiation threshold of PETN with absorptive additives on uniform compression pressure of the sample *Russian Physics Journal* **55** pp 217–219
- [12] Kriger V G, Kalensky A V, Zvekov A A, Zykov I Yu and Nikitin A P 2012 Effect of laser radiation absorption efficiency on the heating temperature of inclusions in transparent media *Combustion, Explosion, and Shock Waves* **48** pp 54–58
- [13] Kalensky A V, Zvekov A A, Anan'eva M V, Zykov I Yu, Kriger V G and Aduiev B P 2014 Influence of Laser Wavelength on the Critical Energy Density for Initiation of Energetic Materials *Combustion, Explosion, and Shock Waves* **50** pp 98–104
- [14] McPeak K M, Jayanti S V, Kress S J, Meyer P S, Iotti S, Rossinelli A and Norris D J 2015 Plasmonic films can easily be better: Rules and recipes *ACS Photonics* **2** pp 326–333
- [15] Larruquert J I, Rodríguez-de Marcos L V, Méndez J A, Martin P J and Bendavid A 2013 High reflectance ta-C coatings in the extreme ultraviolet *Opt. Exp.* **21** pp 27537–27549